

OPTIMIZATION OF MEMORY TASK ALLOCATION IN STOCHASTIC FUNCTIONAL SELF-ORGANIZED SORTING PERFORMED BY COOPERATIVE AUTONOMOUS MOBILE AGENTS

S. A. OPRISAN¹ and P.T. FRANGOPOL²

¹*Department of Psychology, University of New Orleans, New Orleans, LA 70148, U.S.A.*

²*Department of Chemical Physics, "Babes-Bolyai" University, R-3400 Cluj-Napoca, Romania*
(Received July 28, 2003)

Abstract. A team of autonomous mobile agents can coordinate its behavior through a continuous changing environment. The emergent behavior is a distributed sorting and clustering activity based entirely on local information processing. We derived an optimum memory weighting function based on *intermediate steady-states* assumption using angular second-moment (ASM) as optimization criterion.

Key words: self-organizing systems, pattern recognition, simulated annealing, mobile agents

1. INTRODUCTION

The reasons for growing interest in swarm intelligence applications are twofold. Some tasks may be inherently too complex or impossible for a single robot to perform. On the other hand, a swarm of simple robots may also be more flexible without the need to reprogram the robots, and more reliable and fault-tolerant because one or several robots may fail without acting task completion. In addition, self-organization and decentralization made possible via interactions taking place through the environment, point to the possibility of significantly reducing communications between robots. Most contributions to date in swarm intelligent robotics present statistical analyses of the results [2] which, however, do not allow experimenters to identify the system parameters which have influenced the performance. Furthermore, the stochastic nature of the swarm intelligence approach usually leads to high variability in performance, as clearly shown in [12]. Swarm intelligence models can, at least partially, describe the collective activities of social insects, include the formation of trail networks and foraging patterns in many ant species [4,6,7], rhythmical patterns of activity in ants (*Leptothorax*) [3], thermoregulation in clusters of bees [20], the piling of dead bodies by ants (*Pheidole*) [5], larval sorting by ants (*Leptothorax*) [5], or the dynamics of colony development in wasps (*Polistes*) [11]. Self-organization has also been applied to the modeling of the social organization, including hierarchical differentiation [10,18], division of labor [17,18], and age (or temporal) polyethism [19].

In our study, the robots' mission is to search and collect "food-items" in a foraging area and sort them in disjoint piles. A theoretical expression for the time-dependent memory radius, r , for the functional self-organization process [1,8,13,14,15,16] was derived. The optimization procedure is based on intermediate steady states assumption and its validity was numerically tested using the angular second-moment feature as aggregation degree [9].

2. THE MECHANISM OF STOCHASTIC FUNCTIONAL SELF-ORGANIZATION BASED ON MEMORY-WEIGHTED MODEL

Our model is based on the following assumptions:

1. The environment is a two-dimensional periodic lattice with $N_x \times N_y$ sites. The periodic lattice (torus) was considered in order to eliminate the finite size effects.
2. The lattice sites are occupied by *objects* denoted by letters a, b, c and so forth. A free site is occupied by a ϕ -type object.
3. The agents called *robot-like-ant* (RLA)}, move randomly through the lattice. Anytime the RLAs transport an object. The carried object might be of ϕ -type and, therefore, the robot move freely.
4. When a robot moves to a given site, it must decide if there are conditions to put down the carrying object and to pick up the existing one. The swapping condition writes

$$f_\alpha \geq f_\beta, \quad (1)$$

where f_α is the weighted frequency of the carried α -type object and f_β is the corresponding weighted frequency of the encountered β -type object.

Walking through the lattice, every RLA records in its *memory register* the object-types encountered. By analyzing its content, the RLA extracts information about the spatial arrangement of the objects. In the current implementation, a binary string with the following structure characterizes every object-type:

$$S_{\alpha,\tau} : u_{\alpha,1} u_{\alpha,2} \dots u_{\alpha,\tau}, \quad (2)$$

where

$$u_{\alpha,i} = \begin{cases} 1, & \text{if an } \alpha \text{ - type object was encountered at } i \text{ - th step,} \\ 0, & \text{otherwise.} \end{cases} \quad (3)$$

The following conservation rules take place $\sum_{i=1}^{\tau} u_{\alpha,i} = n_{\alpha}$, for any $\alpha = 1, \dots, T$,

where n_{α} is the total number of α -type object encountered and $\sum_{\alpha=1}^T u_{\alpha,i} = 1$, for any $i = 1, \dots, \tau$, where T is the total number of distinct object types.

An important memory register model, proposed by Deneubourg [5], consists in a shift register of fix length with equal weight. As the time passes, the whole record is shifted one place, the older (less significant) record is removed, and on the first (most significant) place enters the new record. Another important memory register model, proposed by Oprisan [1,8,13,14,15,16], uses a first order recurrence to define the actual state of the CA. The main advantage is its computational efficiency and long (temporal) correlation. The computational efficiency reflects in an economic memory allocation: only two real variables must be stored - the previous state of CA and the state associated with the newly encountered object-type. Long (temporal) correlation means that the actual state depends on the whole history of the system's states. Actually, it was proved (see [13,14,15,16]) that there is an intrinsic limit of the temporal correlation imposed by the machine accuracy. However, the temporal length of correlation for the model proposed is orders of magnitude bigger than for the fix number of shift register.

In our weighted memory register, every object-type is characterized, at any instant τ , by a weighted frequency:

$$f_{\alpha}(\tau) = \frac{\sum_{i=1}^{\tau} w(i) u_{\alpha,i}}{\sum_{i=1}^{\tau} w(i)}, \quad (4)$$

where $w(i)$ is an appropriate weighting function. The weighting function is

$$w(i) = \frac{1}{r^{i-1}}, \quad (5)$$

indicating that for $r \gg 1$ the contribution of the τ -th step (with $\tau \gg 1$) to present decision is quite insignificant (*short-type memory*). This choice simulates the long-term memory effect. The limit case $r = 1$ corresponds to an infinite and equally weighted record. When $r < 1$ the contribution of older steps become significant [1,8]. This type of memory function, that enhances the effect of past history, was suggested as a possible microscopic mechanism in a model of metastasis [1,14,15,16].

The above definition of the memory register leads to a first order recursive definition of the weighted memory associated to every object-type [14].

Numerical simulations have shown that the memory radius, (r), should depend on the cluster dimension (i.e. aggregation stage) in order to optimize the computational effort [13,14,15,16]. Thus, clustering process occurs for any $r > 1$ but the speed with which the system reaches his sorted steady state depends sensibly on r : an abruptly decreasing memory radius drives the system into equilibrium state consisting in many small clusters (nonequilibrium state). The present study provides a proper memory radius-time relationship in order to allow sorting and avoid local equilibrium states.

3. RESULTS

3.1. Theoretically derived relationship between memory radius and aggregation stage. The intermediate steady-states hypothesis

The swapping process that take place between n -th and $n+1$ -th computational time lead to

$$f_{\alpha}^n < f_{\beta}^n, f_{\alpha}^{n+1} > f_{\beta}^{n+1}. \quad (6)$$

For simplicity, only two object-types, a , b , were considered. Based on (3), it results $u_{\beta,i}^n = 1 - u_{\alpha,i}^n$, and

$$f_{\beta}^n = \sum_{i=0}^{\tau} \frac{u_{\beta,i}^n}{r^i}. \quad (7)$$

Substituting above relationship into (6), it gives $f_{\alpha}^n < \frac{1}{2} \sum_{i=0}^{\tau} \frac{1}{r^i}$. An "1" bit on the most recent entry of the α -type object binary string forces swapping after $n+1$ time step. Using (4), the swapping condition writes $f_{\alpha}^n < r \left(\frac{1}{2} \sum_{i=0}^{\tau} \frac{1}{r^i} - 1 \right)$, where the following recurrent relationship was used $f_{\alpha}^{n+1} = 1 + f_{\alpha}^n/r$. Summarizing, in the limit of large memory $\tau \rightarrow \infty$, the swapping conditions (6) is:

$$\frac{r(2-r)}{2(r-1)} < f_{\alpha}^n < \frac{r}{2(r-1)}. \quad (8)$$

The aggregation process takes place progressively: starting with a random distribution, first only two-object clusters appear, then only three-object clusters and so forth. This *intermediate steady-states assumption* helps us to establish a

quantitative relationship between the memory radius, (r), and the aggregation stage. For example, after n -th computational step, a two-object cluster appears if, based on (8), the memory radius satisfies $r \in (2^{1/2}, 2)$. For three-object clusters the memory radius must satisfies $r \in (r^{1/3}, r^{1/2})$. Generally, it is straightforward that transition from p -objects clusters steady state to $(p+1)$ -objects clusters requires $r \in (2^{1/(p+1)}, 2^{1/p})$.

To determine how long it will take, in conventional iteration steps, to realize a complete two-objects clusters steady state and then a three-objects one and so on, a mean field view-point was adopted. Let us denote by N_α the number of α -type objects in the lattice and by \sqrt{N} the linear dimension of the square lattice. The mean distance, λ , between the same object-types, for a uniform distribution of the

objects, is given by conservation condition $N_\alpha = \left(1 + \frac{\sqrt{N}}{\lambda}\right)^2$, which implies

$$\lambda = \frac{\sqrt{N}}{2} \frac{1 + \sqrt{4N - 3}}{N_\alpha - 1}. \text{ During the aggregation process the mean-free distance}$$

between the objects increases due to decreasing of the clusters' number. We propose as a conventional iteration time step needed to switch between p and $p+1$ -objects steady clusters a quantity proportional with the sum of the corresponding mean-free distance between the clusters. For example:

$$\lambda^{1 \rightarrow 2} = \frac{\sqrt{N}}{2} \sum_{i=\frac{N_\alpha}{2}}^{N_\alpha} \frac{1}{\sqrt{4i-1}-1},$$

where the superscript $1 \rightarrow 2$ design the initial and, respectively, final aggregation steady states. The proportionality constant depends on the successive identical steps required to visit the same cluster in order to transport them to the nearest neighbor ones. Therefore, taking into account this successive (minimal) number of repetitive visits the above relation can be generalized as follows

$$\lambda^{k \rightarrow k+1} = (2k+1) \frac{\sqrt{N}}{2} \sum_{i=\frac{N_\alpha}{k+1}}^{\frac{N_\alpha}{k}} \frac{1}{\sqrt{4i-1}-1}. \quad (9)$$

Replacing above sum by $\sum_{i=\frac{N_\alpha}{k+1}}^{\frac{N_\alpha}{k}} \frac{1}{\sqrt{4i}}$, valid for $N_\alpha \gg 1$, on the bases of Euler

formula

$$\sum_{i=a}^b f(i) \cong \int_a^b f(x)dx + \frac{1}{2}(f(a) + f(b)) + \frac{1}{12}(f'(b) - f'(a)) + \dots,$$

it results

$$\lambda^{k \rightarrow k+1} \cong (2k+1) \frac{\sqrt{N}}{2} \sum_{i=\frac{N_\alpha}{k+1}}^{\frac{N_\alpha}{k}} \frac{1}{\sqrt{4i}} \cong 2N(2k+1) \frac{\sqrt{k+1} - \sqrt{k}}{\sqrt{k(k+1)}},$$

which simplifies to $k \cong \frac{2N}{\lambda}$.

On the other hand, we previously found that to built clusters with k objects (in the k -objects steady state sorting stage) the memory radius, (r), must lie in the range ($2^{1/(k+1)}, 2^{1/k}$). Therefore, the last two relations give

$$r \propto \exp\left(\frac{\lambda \ln 2}{2N}\right). \quad (10)$$

This is the theoretically derived optimized relationship between the memory radius, r , and the computational time step N .

3.2. Numerical results and the annealing rule

The functional self-organization algorithm above described (see [1,8,13,14] for details) requires a well-defined measure of the aggregation stage. Our choice is a texture analysis using features, which considers that texture-context information is contained in the overall spatial relationship between its gray tone [9]. Let $p(i,j)$ denote the normalized matrix of relative frequencies with which two cells, separated by distance d , occur on the image, one with gray tone i and the other with gray tone j . A relevant feature is *the angular second-moment (ASM)*, which represents a measure of homogeneity of the image.

In a homogeneous image this features has a great values and decrease if the texture become less homogeneous (texture with different clusters):

$$ASM = \sum_{i=1}^{N_g} \sum_{j=1}^{N_g} p(i, j)^2, \quad (11)$$

where N_g is the number of gray levels present in the image under investigation. Numerical simulations demonstrate that the above-defined feature is sensitive to

aggregation stage and offer a quantitative meaning of this fuzzy concept (see Figure 1).

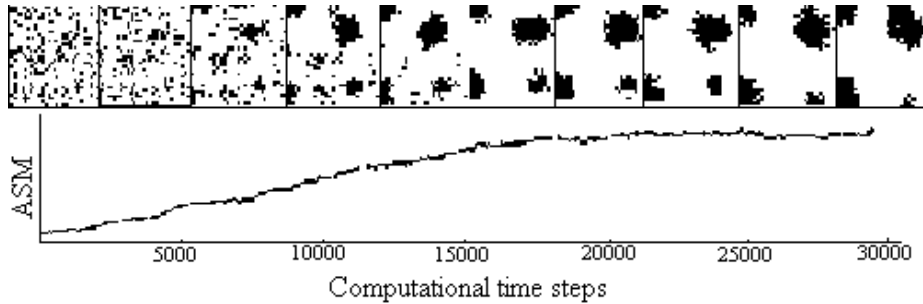


Fig. 1.- Different snapshots are uniformly sampled with 500 time-steps and shown on the top panel. The behavior of the contrast feature against the iteration time-step is plotted (lower panel). Here the environment is a rectangular 100×100 lattice, with 10% black objects' concentration, 40 RLAs and a constant memory radius $r = 1.1$. As the system approaches its final steady state, the contrast feature saturates. The minimum and maximum values were analytically evaluated and, therefore, can be used to measure the distance between the current aggregation stage and the steady state.

Based on the above-defined global measure, we performed extensive numerical simulations to find the optimal time-dependence of the memory radius, (r), in order to validate the theoretical derived relationship (10) and its background hypothesis - the intermediate steady states assumption. We found that at the very beginning of the numerical simulations there is a quasi-linear relationship between the slope of the feature and the time step (see Figure 2). Analyzing Figure 2, we conclude that it is advantageous, in order to reduce the computational effort, to start the numerical simulations with a high value for the memory radius. A high value of the memory radius means a very abrupt decrease of the feature and a rapidly slowing-down of the algorithm. If numerical simulation continues along this path, the system needs a long computation to reach its final steady state. On the other hand, an initial low memory radius determines a slow change of the features but the end of linear region is more closely to its final steady state. Our optimization procedure tries to combine the high speed of the features decreases for initial high memory radius with the lowest quasi steady state at the end of linear region for low memory radius. To determine the limits of the linear domain, which means that for a particular value of the memory radius the algorithm enters the slowing down regime, we performed numerical simulations until the linear correlation coefficient maximizes. At that point the final stage of aggregation was reached, for a particular value of the memory radius (r). We recorded the slope of the contrast feature for that specific memory radius value and the simulations were started over for another value of r .

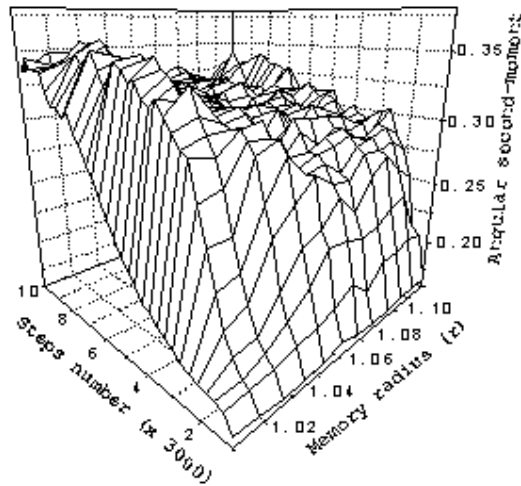


Fig. 2- The 3D plot of the contrast feature against the time-step and memory radius r is shown. With a constant memory radius, a linear dependence of the feature on the time step, at the very beginning of the numerical simulations, can be observed. Decreases of the memory radius determine a decrease of the slope of the feature. On the other hand, the surfaces are highly fractured and, therefore, an appropriate time-dependent memory radius relationship must be chosen in order to avoid trapping the simulation in a local minimum.

Figure 3a summarize the computationally derived optimal relationship between the slope of the contrast feature and the memory radius in order to ensure a minimum computational time. Once the relationship between microscopic control parameter (memory radius r) and the macroscopic measure of aggregation stage (the contrast feature) was established, we get practical instrument to optimize the aggregation process. The computational procedure is as follows. We monitored the slope of the contrast feature and change the memory radius according to computationally derived relationship (see Figure 3a).

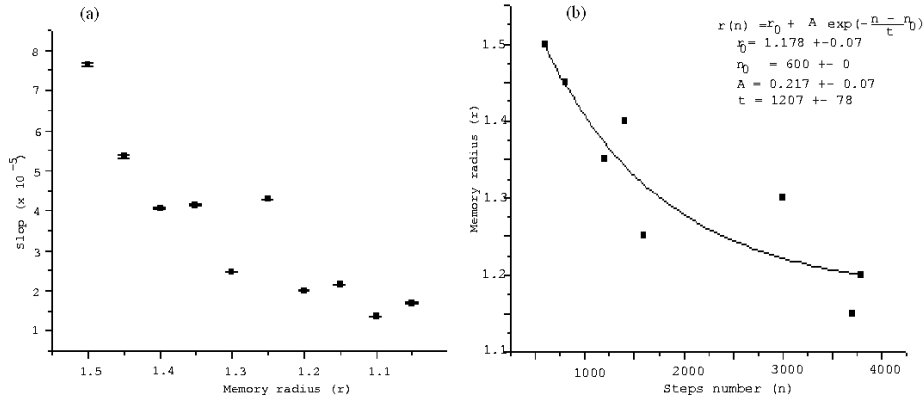


Fig. 3- The plot of the steady slope of contrast feature against the memory radius r (a - left panel). The environment is a rectangular 100 x 100 lattice, with 10% black objects' concentration and 40 RLAs. The chosen slope of the features maximizes the linear correlation coefficient and, therefore, is an indication that the steady state was reached. The plot of the memory radius (r) against the time step (n) when the sorting steady state was reached (b - right panel). The best fit is an exponential decaying function with the indicated parameters.

The plot of the optimally controlled memory radius against the iteration step (see Figure 3b) shows that the interpolation curve (continuous line) agrees with our theoretically derived time-dependent memory radius (see equation (10)).

4. DISCUSSION AND CONCLUSIONS

Previous studies suggested that a realistic approach on the problem of local decision in the aggregation process performed by a team of mobile agents is the first order recurrent memory function [1,8,13,14,15,16]. The present study analyses the dynamical aspects of the memory feature, particularly, its correlation length or *memory radius*. Based on *intermediate steady state* hypothesis we derived a theoretical time-dependent memory radius that leads to a minimum aggregation time. The intuitive idea behind our approach is that each two-, three-, four-, etc. clusters are metastable and the inherent stochastic behavior of the robot-like-ants (RLA) is the mechanism that drives the systems from intermediate (metastable) steady states to a final (stable) steady state. Once we found a time-dependent memory radius, which we thought to be the optimum, the next step was to check our finding using numerical simulation.

On the other hand, using a swarm of robots inspired from social insects behavior has some drawbacks. For example, stagnation is one: because of the lack of a global knowledge, a group of robots may find itself in a deadlock, where it

cannot make any progress. Another problem is to determine how these so-called "simple" robots should be programmed to perform user-designed tasks. The pathways to solutions are usually not predefined but emergent, and solving a problem amounts to finding a trajectory for the system and its environment so that the states of both the system and the environment constitute the solution to the problem: although appealing, this formulation does not lend itself to easy programming. Until now, we implicitly assumed that all robots were identical units: the situation becomes more complicated when the robots have different characteristics, respond to different stimuli, or respond differently to the same stimuli, and so forth; if the body of theory that roboticists can use for homogeneous groups of robots is limited, there is virtually no theoretical guideline for the emergent design and control of heterogeneous swarms.

REFERENCES

1. D. AMARIE, S.A. OPRISAN and M. IGNAT, Random walk systems behavior based on record function, *Physics Letters A*, 254, 112-118, 1999.
2. R. BECKERS, O.E. HOLLAND and J.L. DENEUBOURG, From Local Actions to Global Tasks: Stigmergy and Collective Robotics, *Proceedings of the Fourth International Workshop on the Synthesis and Simulation of Living Systems Artificial Life IV*, 181-189, 1994.
3. B. J. COLE, Short-term activity cycles in ants: generation of periodicity by worker interaction, *The American Naturalist*, 137, 244-259, 1991.
4. J.-L. DENEUBOURG and S. GOSS, Collective patterns and decision making, *Ethology, Ecology and Evolution*, 1, 295-311, 1989.
5. J.-L. DENEUBOURG, S. GROSS, N. FRANKS, A. SANDOVA-FRANKS, C. DETRIAN, L. CHRETIEN, The dynamics of collective sorting : Robot-like ant and ant-like robot, *From Animals to Animats: Proceedings of the First International Conference on Simulation of Adaptive Behavior*, edited by J. A. Meyer and S. W. Wilson (MIT Press, pp. 356-365, 1991).
6. L. EDELSTEIN-KESHET, J. WATMOUGH. and G. B. ERMENTROUT, Trail following in ants: individual properties determine population behaviour, *Behavioral Ecology and Sociobiology*, 36, 119-133, 1995.
7. N. R. FRANKS, The blind leading the blind in army ant raid patterns testing a model of self-organization, *Journal of Insect Behaviour*, 4, 583-607, 1991.
8. C. V. GIURANIUC and S.A. OPRISAN, Short range and long range coupling in stochastic functional self organization, *Physics Letters A*, 259, 334-338, 1999.
9. R. HARALICK, K. SHANMUGAN, I. DISTEIN, *IEEE Transactions on System Man and Cybernetics*, 3, 610-621, 1973.
10. P. HOGEWEG and B. HESPER, Socioinformatic processes: MIRROR modelling methodology, *Journal of Theoretical Biology*, 113, 311-330, 1985.
11. I. KARSAI, Z. PENZES. and J. W. WENZEL, Comb building in social wasps: self-organization and stigmergic script, *Behavioral Ecology and Sociobiology*, 39, 97-105, 1996.
12. C. MELHUIISH, O. HOLLAND, and S. HODDELL, Collective sorting and segregation in robots with minimal sensing(1998): Preprint.
13. S. A. OPRISAN , V. HOLBAN and B. MOLDOVEANU, Functional self-organization performing wide-sense stochastic processes, *Physics Letters A*, 216, 303-306, 1996.
14. S. A. OPRISAN, Convergence properties of the functional self-organization stochastic algorithm, *Journal of Physics A: Mathematical and General*, 31, 8451-8463, 1998.
15. S.A. OPRISAN, A. ARDELEAN and P.T. FRANGOPOL, Self-organization and competition in the immune response to cancer invasion. A phase-orientated computational model of oncogenesis, *Bioinformatics*, 60 (2), 96-100, 2000.

16. S.A. OPRISAN , Theoretical approach on microscopic bases of stochastic functional self-organization. Quantitative measures of the organizational degree of the environment, *Journal of Physics A: Mathematical & General*, 34, 10013–10028, 2001.
17. S. W. PACALA, D. M. GORDON and H. C. J. GODFRAY, Effects of social group size on information transfer and task allocation, *Evolutionary Ecology*, 10, 127-165, 1996.
18. G. THERAULAZ, J. GERVET. and S. SEMENOFF-TIAN-CHANSKY, Social regulation of foraging activities in *Polistes dominulus* Christ: a systemic approach to behavioural organization, *Behaviour*, 116, 292-320, 1991.
19. C. TOFTS and N. R. FRANKS, Foraging for work: how tasks allocate workers, *Animal Behaviour*, 48, 470-472, 1994.
20. J. WATMOUGH, and S. CAMAZINE, Thermoregulation of honeybee clusters, *Journal of Theoretical Biology*, 176, 391-402, 1995.